

Synthesis, Structure and Conformation of Partially-Modified Retro- and Retro-Inverso ψ [NHCH(CF₃)]Gly Peptides

Alessandro Volonterio,^{*[b]} Stefano Bellosta,^[c] Fabio Bravin,^[b] Maria Cristina Bellucci,^[d] Luca Bruché,^[b] Giorgio Colombo,^[e] Luciana Malpezzi,^[b] Stefania Mazzini,^[d] Stefano V. Meille,^[b] Massimiliano Meli,^[e] Carmen Ramírez de Arellano,^[f] and Matteo Zanda^{*[a]}

Abstract: Partially modified retro- (PMR) and retro-inverso (PMRI) ψ [NHCH(CF₃)]Gly peptides, a conceptually new class of peptidomimetics, have been synthesized in wide structural diversity and variable length by aza-Michael reaction of enantiomerically pure α -amino esters and peptides with enantiomerically and geometrically pure *N*-4,4,4-trifluorocrotonoyl-oxazolidin-2-ones. The factors underlying the observed moderate to good diastereocontrol have been investigated. The conformations of model PMR- ψ [NHCH(CF₃)]Gly tripeptides have been studied in solution by ¹H NMR spectroscopy supported by MD calculations, as well as in the solid-state by X-ray diffraction. Remarkable stability of turn-like conformations, comparable to that of parent malonyl-based retro-

peptides, was evidenced, as a likely consequence of two main factors: 1) severe torsional restrictions about sp³ bonds in the [CO-CH₂-CH(CF₃)-NH-CH(R)-CO] module, which is biased by the stereoelectronically demanding CF₃ group and the R side chain; 2) formation of nine-membered intramolecularly hydrogen-bonded rings, which have been clearly detected both in CHCl₃ solution and in some crystal structures. The former factor seems to be more important, as turn-like conformations were found in the solid-state even in the absence of intramolecular hydrogen bonding. The relative configuration of

the -C*H(CF₃)NHC*H(R)- stereogenic centers has a major effect on the stability of the turn-like conformation, which seems to require a *syn* stereochemistry. X-ray diffraction and ab initio computational studies showed that the [-CH(CF₃)NH-] group can be seen as a sort of hybrid between a peptide bond mimic and a proteolytic transition state analogue, as it combines some of the properties of a peptidyl -CONH- group (low NH basicity, CH(CF₃)-NH-CH backbone angle close to 120°, C-CF₃ bond substantially isopolar with the C=O) with some others of the tetrahedral intermediate [-C(OX)(O⁻)NH-] involved in the protease-mediated hydrolysis reaction of a peptide bond (high electron density on the CF₃ group, tetrahedral backbone carbon).

Keywords: conformation analysis • fluorine • Michael addition • peptidomimetics

Introduction

Peptides are essential to virtually every biochemical process but their low bioavailability, which is principally a conse-

quence of fast in vivo degradation by proteolytic enzymes, represents a serious pharmacological drawback.^[1] The need of drug-like molecules retaining both activity and potency of the parent peptides, while at the same time much more stable and

[a] Dr. M. Zanda
C.N.R.—Istituto di Chimica del Riconoscimento Molecolare (ICRM)
Sezione “A. Quilico”, via Mancinelli 7
20131 Milano (Italy)
Fax: (+39) 02 23993080
E-mail: matteo.zanda@polimi.it


[b] Dr. A. Volonterio, F. Bravin, Prof. Dr. L. Bruché, Dr. L. Malpezzi,
Prof. Dr. S. V. Meille
Dipartimento di Chimica, Materiali ed Ingegneria Chimica “G. Natta”
Politecnico di Milano
via Mancinelli 7, 20131 Milano (Italy)

[c] Dr. S. Bellosta
Dipartimento di Scienze Farmacologiche
Università degli Studi di Milano
via Balzaretto 9, 20133 Milano (Italy)

[d] Dr. M. C. Bellucci, Dr. S. Mazzini
Dipartimento di Scienze Molecolari Agroalimentari
Università degli Studi di Milano
Via Celoria 2, 20133 Milano (Italy)

[e] Dr. G. Colombo, M. Meli
C.N.R.—ICRM, Sezione Milano-1
via M. Bianco 9, 20131 Milano (Italy)

[f] Prof. Dr. C. Ramírez de Arellano
Departamento de Química Orgánica
Facultad de Farmacia, Universidad de Valencia
46100 Burjassot, Valencia (Spain)

 Supporting information for this article is available on the WWW under <http://www.chemeurj.org/> or from the author.

orally active, has been a major driving-force for the development of a variety of peptide mimics. Two very attractive ways of generating bio-active peptide mimics with improved biostability are: a) to replace a peptide bond with a surrogate unit X, which is usually symbolized as $\psi(X)$;^[2] b) to reverse all or some of the peptide bonds (NH-CO instead of CO-NH) giving rise to the so called retro- or partially-modified-retro (PMR) peptides, respectively.^[3, 4] When the stereochemistry of one or more amino acids of the reversed segment is inverted, the resulting pseudo-peptide is termed as retro-inverso. A malonic unit is classically incorporated to provide partially-modified retro-peptides, while the direction can be restored incorporating an additional *gem*-diaminoalkyl unit.

Recently, we communicated a new strategy for generating peptidomimetic sequences, based on the idea of combining both the “surrogate-unit” and the “direction-reversal” strategies in a novel class of pseudo-peptides with a $\psi[\text{NHCH}(\text{CF}_3)]$ instead of the $\psi(\text{NHCO})$ unit featured by retro-peptides (Figure 1).^[5]

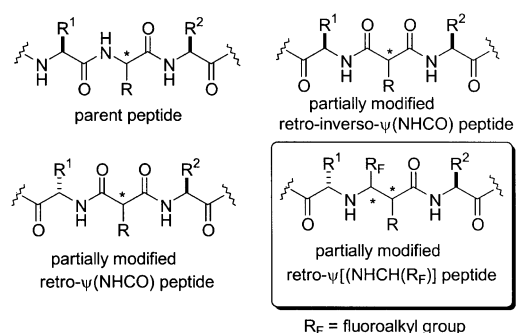


Figure 1. Conventional retro- and retroinverso peptides, and $\psi[\text{NHCH}(\text{CF}_3)]$ retropeptides.

A first intuitive consequence of this structural modification is that the symmetry of conventional malonyl PMR peptides is broken, resulting in the generation of two families of regioisomeric PMR- $\psi[\text{NHCH}(\text{CF}_3)]$ and $-\psi[\text{CH}(\text{CF}_3)\text{NH}]$ peptides (Figure 2),^[6] each one existing in two epimeric forms at the CF_3 -substituted carbon. In this way a great diversity of structurally related, potentially bioactive molecules can be created.^[7]

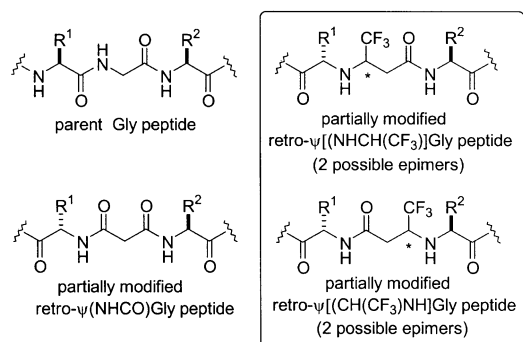


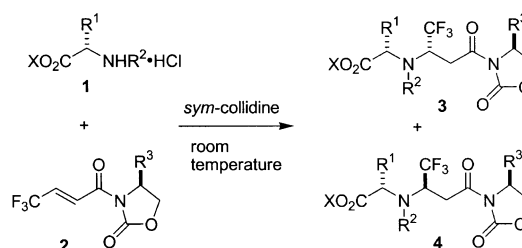
Figure 2. Different isomers of $\psi[\text{NHCH}(\text{CF}_3)]\text{Gly}$ - and $\psi[\text{CH}(\text{CF}_3)\text{NH}]\text{Gly}$ retropeptides.

Further important biological and physicochemical features are expected to arise from the presence of the $[\text{CH}(\text{CF}_3)\text{NH}]$ group. For example, the $\psi[\text{NHCH}(\text{CF}_3)]$ surrogate should be very stable toward proteolytic degradation. Furthermore, the stereoelectronically demanding CF_3 group is expected to constraint the molecule; this limits the number of accessible conformational states and lead to peptidomimetics displaying well-defined conformational motifs. Last but not least, it should modify the binding properties of the parent peptide, changing the hydrogen bonding or coordinative features of the ligand in the putative receptor sites.^[8]

We now report in full on: 1) the solution-phase chemistry which leads to PMR and PMRI $\psi[\text{NHCH}(\text{CF}_3)]\text{Gly}$ peptides ($\text{R}=\text{H}$ in Figure 1), 2) the results of NMR, molecular modelling and X-ray studies on their propensity to assume turn-like conformations in solution and in the solid state, and 3) the structural properties of the $[\text{NHCH}(\text{CF}_3)]$ module using X-ray diffraction and ab initio calculations to characterize its molecular electrostatic potential surface.

Results and Discussion

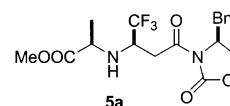
Chemistry: We envisaged a synthetic approach to the $\psi[\text{NHCH}(\text{CF}_3)]$ -containing dipeptide units involving aza-Michael reaction of a series of *L*- α -amino esters **1** (Scheme 1) with enantiomerically and geometrically pure Michael acceptors (*S,E*)-**2**, prepared according to literature methods.^[9]



Scheme 1. Aza-Michael reaction with amino-ester nucleophiles **1**.

This reaction is extraordinarily simple and efficient, if one considers that examples of aza-Michael reactions involving chiral α -amino esters and 4-substituted Michael acceptors are very scarce in the literature.^[10] Pseudo-dipeptides **3** were formed in excellent yields simply by mixing the hydrochlorides, or PTSA salts, **1** (2 equiv) with (*S,E*)-**2** and *sym*-collidine (TMP) (4 equiv) in the appropriate solvent, and stirring at room temperature for 16–88 hours (Table 1).^[11] The solvent has a strong influence on stereoselectivity, as shown by experiments carried out on the model reaction between *L*-**1a** and **2a**. The best results were obtained in CH_2Cl_2 (entry 1), while a substantial drop of *de* was observed with more polar solvents such as ethanol, acetonitrile, THF, DMF or mixtures (entries 2–5). The base also plays an active role, as demonstrated by the fact that the use of DABCO (both in CH_2Cl_2 and toluene), instead of TMP, accelerates the reaction of **1b** with **2a** but lowers the *de* of the product **3c** (entries 9 and 10) in comparison with TMP (entry 8). In the absence of a base (entry 11), namely pre-generating the free α -amino ester

from the hydrochloride by treatment with NaHCO_3 , the diastereoselectivity was similar to that achieved with TMP. In the light of these results, CH_2Cl_2 and TMP were used as, respectively, the solvent and the base of choice for the preparation of pseudo-dipeptides **3a–l**. The facial diastereoselectivity of these reactions is mainly controlled by the nucleophiles **1**. In fact, in all cases L-configured **1** (Scheme 1 and Table 1, entries 1–20) attack preferentially the *Si* face of (*S*)-**2a** producing new (*S*)-centers, whereas enantiomeric D-Ala-OMe **1a** (entry 23) attacks the *Re* face producing the (*R*)-configured diastereomer **5a**, although with lower diastereocontrol (mismatch).^[12] Moreover, compound **3e** was produced with good diastereocontrol when L-Val-OBn **1b** was reacted with the achiral Michael-acceptor **2c** (entry 14), while achiral H-Gly-OEt **1g** (entry 21) and Bn-Gly-OEt **1h** (entry 22) added to (*S*)-**2a** without stereocontrol, affording equimolar mixtures of **3k** and **3l**, respectively. It is therefore apparent that the stereoelectronic features of the α -amino ester R^1 side chain have a major impact on the degree of diastereoselectivity, which follows the trend *iPr* > *iBu* > Me > Bn > H (*de* up to 78% in the case of **3d**, entry 13). Modest *de* was obtained with the cyclic α -amino ester L-Pro-OBn **1f** (entry 20), but the reaction occurred also in this case with very good yield. On the other hand, the R^3 substituent on the oxazolidinone stereocenter has a lower effect on the stereoselectivity. In fact, (*S*)-configured products **3d** ($\text{R}^3 = i\text{Pr}$, entry 13), **3c** ($\text{R}^3 = \text{Bn}$, entry 11) and **3e** ($\text{R}^3 = \text{H}$, entry 14) were obtained from L-Val-OBn **1b** in 78, 72 and 65% *de*, respectively, with little variation and the same sense of facial selectivity. No meaningful effect is exerted by the X group of the nucleophile, as shown by the fact that L-Phe-OBn (**1f**, entry 15) and L-Phe-OBu (**1g**, entry 16) added to **2a** with nearly identical diastereocontrol (43 and 45%, respectively).



The results described above can be rationalized if one considers that in the absence of chelating agents *N*-(*E*)-enoyloxazolidin-2-ones **2** exist in *transoid* conformation (as portrayed throughout the paper),^[13] with the R^3 substituent pointed away from the $\text{C}=\text{C}$ bond, thus exerting little control of the facial selectivity. In contrast, the R^1 side chain of α -amino esters **1** should be spatially close to the forming stereogenic center in the transition state, therefore its influence is much more important. Chelation with Lewis acids for biasing the oxazolidin-2-ones **2** in *cisoid* conformation was tried with little success. For example, treatment of **2a** with $\text{Sc}(\text{OTf})_3$ (entry 12),^[14] followed by addition of L-**1c** and TMP, produced **3d** in 58% *de* and $\approx 85\%$ yield (determined by ^{19}F NMR of the crude reaction mixture) after 30 h at RT. The reaction time had no effect on diastereoselectivity, in fact **3h** was formed from **1e** and **2a** with the identical 50% *de* after 16 h (ca. 50% conversion, entry 18) or after 88 hours as well (entry 17), as shown by NMR of the crude reaction mixture. This strongly supports the conclusion that adducts **3** are formed irreversibly, and the stereochemical outcome is under kinetic control.

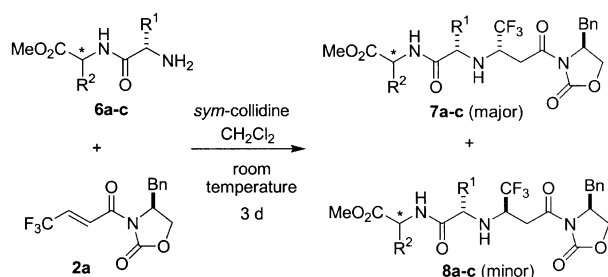
It is worth noting that stereocontrol is totally absent in the aza-Michael reaction of L-Ala-OMe **1a** with methyl 4,4,4-trifluorocrotonate, which was chosen initially as the Michael acceptor, and the reaction is much slower (one month, RT). This is likely to be a consequence of the lower conformational rigidity and electrophilicity of 4,4,4-trifluorocrotonate with respect to the oxazolidinone acceptors **2**.

Table 1. Aza-Michael reaction with amino-ester nucleophiles **1**.

Entry	Major product	AA Acceptor	Oxazolidinones	R^1	R^2	R^3	X	Solvent	Base	<i>t</i> [h]	Yield [%] ^[c]	<i>de</i> [%] ^[d]
1	3a	1a	2a	Me	H	Bn	Me	CH_2Cl_2	TMP	16	90	50
2	3a	1a	2a	Me	H	Bn	Me	EtOH	TMP	16	80	20
3	3a	1a	2a	Me	H	Bn	Me	MeCN	TMP	40	80	31
4	3a	1a	2a	Me	H	Bn	Me	THF/DMF 4:1	TMP	40	n.d. ^[b]	26
5	3a	1a	2a	Me	H	Bn	Me	PhH/DMF 4:1	TMP	40	> 98	29
6	3b	1a	2b	Me	H	<i>iPr</i>	Me	CH_2Cl_2	TMP	64	91	60
7	3c	1b	2a	<i>iPr</i>	H	Bn	Bn	CH_2Cl_2	TMP	64	92	72
8	3c	1b	2a	<i>iPr</i>	H	Bn	Bn	CH_2Cl_2	TMP	6.5	41 ^[d]	72
9	3c	1b	2a	<i>iPr</i>	H	Bn	Bn	CH_2Cl_2	DABCO	6.5	58 ^[d]	69
10	3c	1b	2a	<i>iPr</i>	H	Bn	Bn	toluene	DABCO	6.5	65 ^[d]	68
11	3c	1b	2a	<i>iPr</i>	H	Bn	Bn	CH_2Cl_2	None	60	> 98	72
12 ^[e]	3c	1b	2a	<i>iPr</i>	H	Bn	Bn	CH_2Cl_2	TMP	60	85	58
13	3d	1b	2b	<i>iPr</i>	H	<i>iPr</i>	Bn	CH_2Cl_2	TMP	68	> 98	78
14	3e	1b	2c	<i>iPr</i>	H	H	Bn	CH_2Cl_2	TMP	68	90	65
15 ^[a]	3f	1c	2a	Bn	H	Bn	Bn	CH_2Cl_2	TMP	24	78	43
16	3g	1d	2a	Bn	H	Bn	<i>t</i> -Bu	CH_2Cl_2	TMP	60	> 98	45
17 ^[a]	3h	1e	2a	<i>iBu</i>	H	Bn	Bn	CH_2Cl_2	TMP	88	> 98	50
18	3h	1e	2a	<i>iBu</i>	H	Bn	Bn	CH_2Cl_2	TMP	16	50 ^[d]	50
19	3i	1e	2b	<i>iBu</i>	H	<i>iPr</i>	Bn	CH_2Cl_2	TMP	68	> 98	60
20	3j	1f	2a	-(CH_2) ₃ -	H	Bn	Bn	CH_2Cl_2	TMP	40	> 98	29
21	3k	1g	2a	H	H	Bn	Et	CH_2Cl_2	TMP	40	> 98	< 5
22	3l	1h	2a	H	Bn	Bn	Et	CH_2Cl_2	TMP	72	70 ^[d]	< 5
23	5a	D-1a	2a	Me	H	Bn	Me	CH_2Cl_2	TMP	16	> 98	31

[a] PTSA salt of the amino acid was used. [b] Not determined. [c] Overall isolated yield of both diastereomeric products, unless otherwise stated. [d] Determined by 500 MHz ^1H and ^{19}F NMR. [e] Oxazolidinone **2a** was prior treated with $\text{Sc}(\text{OTf})_3$ in CH_2Cl_2 at RT for 30 min.

We next explored the viability of the method for preparing longer PMR and PMRI ψ [NHCH(CF₃)]Gly peptides by using *N*-terminally unprotected peptides as nucleophiles. Satisfactorily, dipeptides **6a–c** (Scheme 2) reacted with **2a** affording in excellent yields and good stereocontrol the tripeptide



Scheme 2. Aza-Michael reaction with dipeptide nucleophiles **6**.

mimics **7a–c** (Table 2). It is worth noting that while, in analogy with simple α -amino esters **1**, H-Val-Ala-OMe **6b** (entry 2) added more stereoselectively (70% *de*) than H-Phe-Ala-OMe **6a** (46% *de*, entry 1), we observed an unexpectedly strong effect by the remote stereocenter of the second amino-acid residue. In fact, the dipeptide H-Val-D-Ala-OMe **6c** (entry 3) scored a much lower diastereocontrol than **6b**, affording **7c** in 54% *de*.

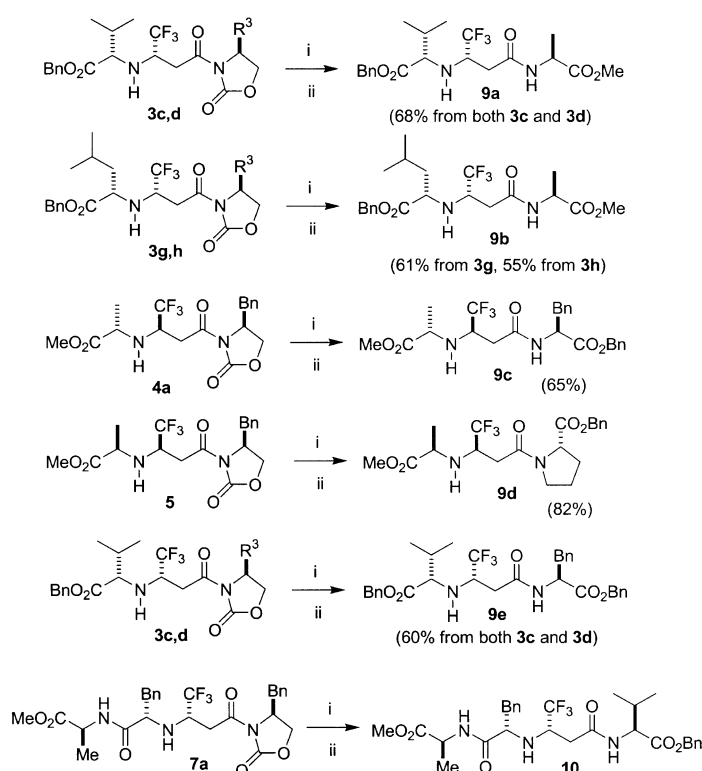
Table 2. Aza-Michael reaction with dipeptide nucleophiles **6**.

Entry	Product	Dipeptide	R ¹	R ²	Yield [%] ^[a]	<i>de</i> [%] ^[b]
1	7a	6a	Bn	L-Me	> 98	46
2	7b	6b	<i>i</i> Pr	L-Me	90	70
3	7c	6c	<i>i</i> Pr	D-Me	> 98	54

[a] Overall isolated yield of both diastereomeric products. [b] Determined by 500 MHz ¹H and ¹⁹F NMR.

With a number of PMR ψ [NHCH(CF₃)]Gly peptides at hand we addressed the chemoselective cleavage of the oxazolidinone auxiliary. This result was achieved in 55–82% yields upon treatment of the oxazolidinone pseudo-peptides **3–7** (Scheme 3) with LiOH/H₂O₂ (30 min, 0 °C).^[15] The resulting pseudo-di- and tri-peptides with a terminal CO₂H group were purified by FC, then coupled with another α -amino ester (HATU/HOAt, *sym*-collidine, DMF). The final PMR and PMRI tripeptides **9a–e** and tetrapeptide **10**, orthogonally protected at the carboxy end groups (except **9e**) and therefore suitable for further selective elongation, were obtained in quantitative yields, often as solid materials.^[16]

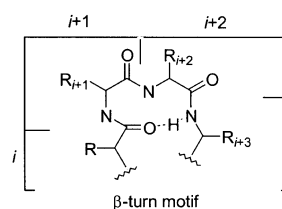
A very interesting feature of PMR ψ [NHCH(CF₃)]Gly peptides **3–10** is their weakly basic nature, which is due to the presence of the strongly electron-withdrawing CF₃ in the α -position to the amino group. As a matter of fact, PMR ψ [NHCH(CF₃)]Gly peptides **3–10** did not form stable salts with trifluoroacetic acid or 2*N* hydrochloric acid, as assessed by ¹H and ¹⁹F NMR spectroscopy.^[17] In terms of basicity, the [NHCH(CF₃)] moiety resembles a retropeptide unit [NHCO] more closely than a conventional secondary amine moiety.



Scheme 3. i) LiOH, H₂O₂; ii) HATU/HOAt, *sym*-collidine, DMF, α -amino ester.

Bio-assays: Within the frame of an ongoing program aimed at the identification of fluorinated peptide mimics for inhibition of matrix metalloproteinases (MMPs), the three model compounds **9b,c,e** were randomly chosen to study their effect on MMP-9 (gelatinase B) expression and activity in human macrophages. In contrast with PMR ψ [NHCH(CF₃)]Gly-peptidyl hydroxamates,^[7c] some of which showed moderate activity, the three assayed molecules showed negligible activity, confirming the well known importance of the terminal hydroxamate function for MMPs inhibition.

Secondary structure of PMR ψ [NHCH(CF₃)]Gly peptides: β -Turns are one of the three major structural elements of peptides and proteins. A β -turn is characterized by the presence of a ten-membered intramolecularly hydrogen-bonded (C=O...H–N) ring involving four amino-acid residues (from *i* through the *i*+3 positions).^[18] It has been shown



that very simple PMR-peptides, such as the triamide **11** (Figure 3), adopt turn-like nine-membered folding patterns

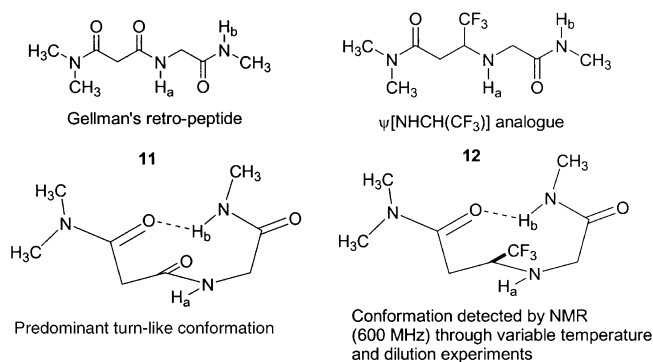
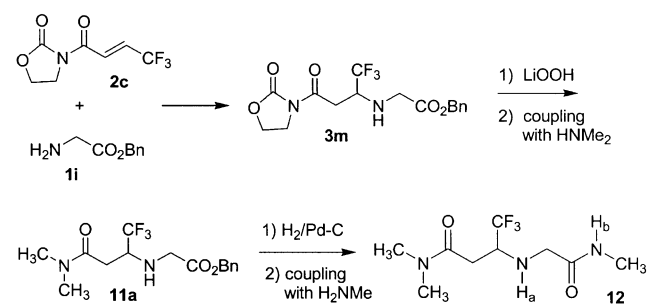


Figure 3. Conformations of Gellman's and ψ [NHCH(CF₃)]Gly peptides.

with an intramolecular N–H...O=C hydrogen bond in the solid state, as well as in low-polarity solvent solutions.^[19]

As a starting point of our investigation on the properties of PMR ψ [NHCH(CF₃)]Gly peptides, we decided to assess whether some conformational analogies exist with the unfluorinated parent molecules. Racemic ψ [NHCH(CF₃)]-diamide **12** (Figure 3) was synthesized in good overall yield by aza-Michael of H-Gly-OBn (**1i**) with the achiral acceptor **2c** (Scheme 4), followed by a standard reaction sequence performed on the adduct **3m**.



Scheme 4. Synthesis of the model ψ [NHCH(CF₃)]-diamide **12**.

In a weakly hydrogen bonding solvent, such as CDCl₃, both the absolute value and the temperature dependence of an amide proton chemical shift provide important structural information. To assess whether the amide NH_b proton of **12** is involved in hydrogen bonding, we first investigated the “reduced temperature coefficient” $\Delta\delta/\Delta T$.^[20] ¹H NMR variable temperature studies from 293 to 213 K, performed on a 3 mM solution of **12** in CDCl₃, showed that the chemical shifts of the amide protons NH_b moved downfield of 0.81 ppm, with a $\Delta\delta/\Delta T$ 0.0101 (see Figure 4). This very high $\Delta\delta/\Delta T$ ratio strongly suggests that the NH_b proton forms hydrogen bonds of increasing stability as the temperature is lowered.

In order to determine if such chemical shift variations were due to the formation of intra- or intermolecular hydrogen bonds, another series of ¹H NMR experiments was performed at 0.05 mM of **12** in CDCl₃, and the spectra were acquired at different temperatures ranging from 293 to 213 K. In the range between 293 and 273 K the NH_b chemical shift of **12** moved upfield of 0.1 ppm with the dilution in comparison with the 3 mM solution (see Figure 4), indicating a partial disruption of hydrogen bonds. This strongly suggests that intermo-

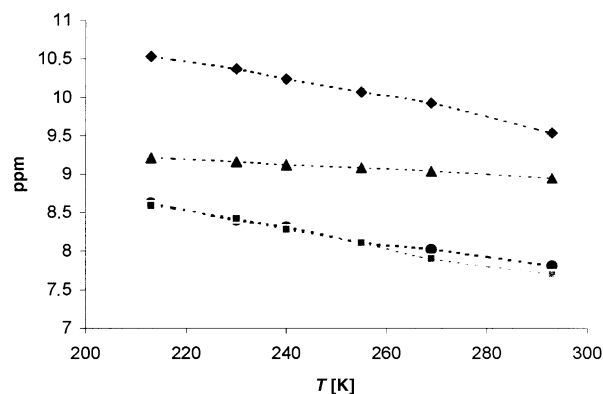
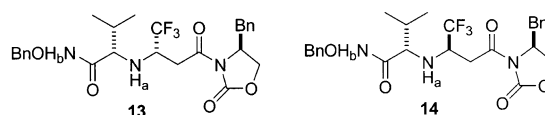


Figure 4. Amide proton (NH_b) NMR chemical shifts of **12** (●, *c* = 3.0 mM; ■, *c* = 0.05 mM), **13** (◆, *c* = 3.0 mM) and **14** (▲, *c* = 3.0 mM) in CDCl₃ solutions as a function of temperature.

lecular hydrogen bonds are involved in this range of temperatures. In contrast, at lower temperatures (from 263 to 213 K) the NH_b chemical shift did not change significantly with dilution (Figure 4). A very high $\Delta\delta/\Delta T$ 0.0111 was also observed at this concentration. The data above can be interpreted in terms of formation of a more stable intramolecularly hydrogen-bonded folded structure of **12** at low temperature (see Figure 3), in analogy with Gellman's unfluorinated PMR-peptide **11**.

However, 2D ROESY experiments performed on **12** at both 213 and 293 K did not show NOE interactions that could unambiguously confirm the presence of a folded conformation, because also the distance values of the extended structure are within 5 Å.

Next, in order to investigate the effect of the configuration of the CF₃-substituted stereogenic center on the conformation of PMR ψ [NHCH(CF₃)]Gly peptides in solution, we selected the two diastereomeric *O*-Bn PMR ψ [NHCH(CF₃)]Gly-peptidyl hydroxamates **13** and **14**.^[21]



In fact, we have recently shown via X-ray diffraction that in the solid state **13** displays a hydrogen-bonded turn-like conformation (Figure 5) closely resembling that of unfluorinated PMR peptides.^[19] ¹H NMR variable temperature experiments (from 293 to 213 K), performed on 3 mM solutions of **13** and **14** in CDCl₃ showed, respectively, a 0.99 ppm ($\Delta\delta/\Delta T$ 0.0124) and 0.26 ppm ($\Delta\delta/\Delta T$ 0.00325) deshielding for the NH_b protons (see Figure 4).^[22] It is also immediately apparent that **13** exhibits NH_b chemical shifts downfield at all temperatures with respect to **14**, which in turn was always deshielded with respect to **12**. In solution, in a regime of fast exchange, the observed chemical shifts are averages of the shifts of the non-hydrogen bonded and hydrogen bonded species, so it is possible qualitatively to conclude that: 1) the NH_b protons of both **13** and **14** are more involved in hydrogen bonding than the NH_b of **12**; 2) the NH_b protons of both **13** and **14** form hydrogen bonds of increasing

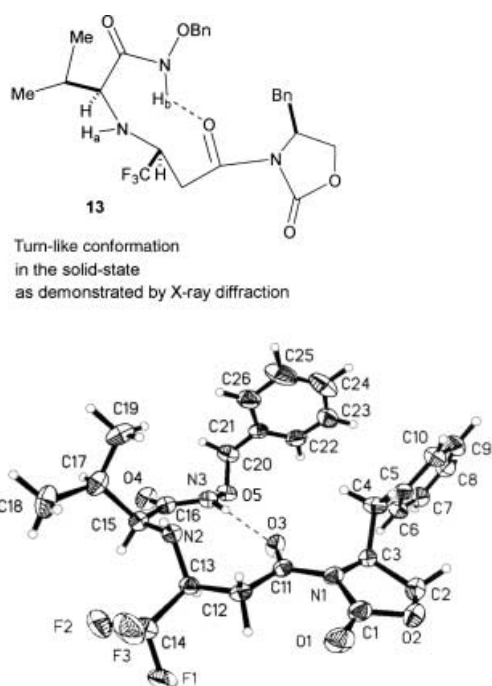


Figure 5. Crystal conformation of PMR ψ [NHCH(CF₃)]Gly-peptidyl hydroxamates **13**.

stability as the temperature is lowered; 3) the upfield shift and the smaller variation of chemical shift for the NH_b proton of **14** are consistent with, respectively, a lower proportion of hydrogen bonding and a lower dependence of its folding pattern on the temperature in comparison with its diastereoisomer **13**. In order to assess whether such hydrogen bonding is inter- or intramolecular, concentration-dependence experiments (not shown in Figure 4) were carried out: the NH_b chemical shifts of **13** and **14** did not change with dilution (down to 0.05 mM) at constant temperature, thus demonstrating that the hydrogen bonds are predominantly intramolecular.

Actually the NOE data must be considered as the average of the interactions occurring for many conformations. In the case of **13** 2D ROESY spectra performed at 213 and 293 K, allowed to obtain *specific* NOE interactions (see Figure 6 and

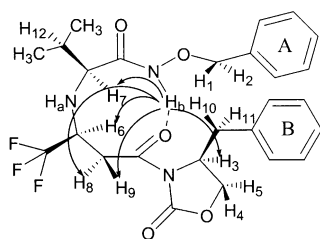


Figure 6. The arrows indicate the experimental NOEs determining the folded structure of **13**.

Table 3) that unambiguously confirmed that in addition to the extended conformations, this compound adopts stable folded structures in solution. In particular, NH_b shows contacts with H-6, H-7 (strong interactions), H-3, H-8 and H-9 protons (weak interactions). It is interesting to note that the folded

Table 3. Intramolecular NOE interactions and interproton distances values [Å] for **13**.

Experimental NOE	Model distances
NH _b ...H-1 (<i>pro R</i>)	2.58
NH _b ...H-2 (<i>pro S</i>)	3.14
NH _b ...H-3	4.36
NH _b ...H-6	2.91
NH _b ...H-7	3.48
NH _b ...H-8 (<i>pro R</i>)	4.53
NH _b ...H-9 (<i>pro S</i>)	4.12
NH _b ...H-12	4.04
NH _b ...NH _a	2.06
NH _b ...CH ₃ (<i>pro S</i>)	3.49
NH _b ...CH ₃ (<i>pro R</i>)	4.84
NH _b ...Phe(A) (<i>pro S</i>)	4.75
Phe(A)...H-1 (<i>pro R</i>)	2.40
Phe(A)...H-2 (<i>pro S</i>)	3.49
Phe(B)...CH ₃ (<i>pro S</i>)	4.05
Phe(B)...H-12	4.97
Phe(B)...NH _a	3.59
Phe(B)...H-3	4.34
Phe(B)...H-4 (<i>pro R</i>)	4.50
Phe(B)...H-5 (<i>pro S</i>)	4.88
Phe(B)...H-10 (<i>pro R</i>)	2.44
Phe(B)...H-11 (<i>pro S</i>)	3.63
H-1...H-2	1.76
H-1 (<i>pro R</i>)...H-6	4.23
H-3...H-4 (<i>pro R</i>)	2.80
H-3...H-5 (<i>pro S</i>)	2.34
H-3...H-10 (<i>pro R</i>)	3.12
H-3...H-11 (<i>pro S</i>)	2.59
H-4...H-5	1.76
H-4 (<i>pro R</i>)...H-11 (<i>pro S</i>)	2.39
H-5 (<i>pro S</i>)...H-11 (<i>pro S</i>)	3.43
H-4 (<i>pro R</i>)...H-10 (<i>pro R</i>)	2.77
H-6...H-8 (<i>pro R</i>)	2.64
H-6...H-9 (<i>pro S</i>)	3.58
H-8...H-9	1.75
H-7...CH ₃ (<i>pro R</i>)	2.70
H-7...CH ₃ (<i>pro S</i>)	3.52
H-7...NH _a	2.99
H-7...H-12	2.43
H-6...NH _a	2.63
H-10...H-11	1.74
H-8 (<i>pro R</i>)...NH _a	3.53
H-9 (<i>pro S</i>)...NH _a	2.52
H-12...NH _a	3.84
H-12...CH ₃ (<i>pro R</i>)	2.14
H-12...CH ₃ (<i>pro S</i>)	2.13
NH _a ...CH ₃ (<i>pro R</i>)	3.64
NH _a ...CH ₃ (<i>pro S</i>)	2.96
CH ₃ ...CH ₃	2.51

conformation is already present at 293 K, indicating a strong natural tendency of this molecule to bend.

2D ROESY experiments performed under the same experimental conditions on **14** showed some differences concerning the NOE, in comparison with its diastereoisomer **13**. In particular, we observed that the NOE contacts between the NH_b amide proton and H-6, H-7 (*strong interactions*) are preserved, while the NOE between NH_b and the H-3 proton here is lacking. Weaker contacts of NH_b with H-8 and H-9 with respect to **13** were also detected. Thus, one can say that also the hydroxamate **14** shows a certain tendency to fold in solution, but the turn-like conformation featuring a C=O...H_b-N intramolecular hydrogen bond here is less populated.

This result is in accord with the minor chemical shift variation found for the NH_b (see Figure 4), which confirms that the molar fraction of the hydrogen bonded conformations is lower. These findings evidence that the configuration of the CF_3 -substituted carbon has an important effect on the folding of PMR $\psi[\text{NHCH}(\text{CF}_3)]\text{Gly}$ peptides in solution.^[23]

Because of the large conformational motions expected for the **13**, MD simulations were performed without experimental constraints, which provided a set of structures that, after minimisation, converge in many folded structures at low energy. The conformation reported in Figure 7 ($E = 136 \text{ kcal mol}^{-1}$) features the best agreement with the experimental NOE data (Table 3) and presents an nine-membered

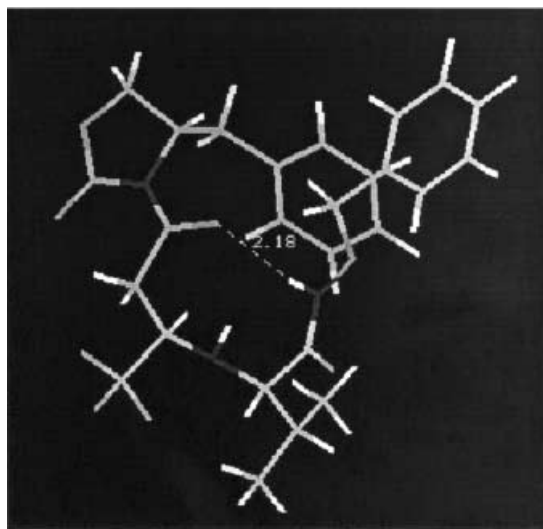


Figure 7. Conformation of **13** obtained from molecular modelling.

intramolecularly hydrogen bonded ring with a $\text{C}=\text{O}\cdots\text{H}-\text{N}$ distance of 2.18 \AA .^[24] It is worth noting that the bond angle $(\text{CF}_3)\text{CH}-\text{NH}-\text{C}$ is 118.54° predicting a widened geometry of the amine nitrogen atom N4 that is confirmed by experimental evidence (see below). The model distances reported in Table 3 are in good agreement with the solid state, where the X-ray analysis of this compound showed a folded structure with a distance of 1.95 \AA for the hydrogen bond.^[7c]

Structural properties of the $\psi[\text{NHCH}(\text{CF}_3)]$ unit: A study on the structural and geometric properties of the $\psi[\text{NHCH}(\text{CF}_3)]$ group was carried out by means of X-ray diffraction and computational methods, also with the aim of understanding the role of such units in promoting turn-like structures in PMR $\psi[\text{NHCH}(\text{CF}_3)]\text{Gly}$ peptides.

Analysis of the X-ray structures of **3a**, **9a**, **9c** (Figure 8)^[25] and of the known hydroxamate **13** (Figure 5)^[7c] highlighted the distortion of the sp^3 nitrogen atom N2: the $\text{C13}-\text{N2}-\text{C15}$ angle is in fact close to 120° (see Table 4). This value is comparable with that found in amides and somewhat larger than the already wide average of 116.65° determined for 203 secondary amine structures having the appropriate structural features found in a Cambridge Structural Database search.^[26] The $\text{N2}-\text{C13}$ and $\text{N2}-\text{C15}$ bond lengths are very similar in **3a**, **9a** and **9c** and invariably shorter than the average value of

Table 4. Selected geometrical parameters for **3a**, **9a**, **9c** and **13**.

	3a	9a	13	9c
bond lengths				
N2–C13	1.453(3)	1.444(3)	1.449(3)	1.427(6)
N2–C15	1.466(3)	1.450(3)	1.462(3)	1.441(6)
C12–C13	1.522(3)	1.519(4)	1.522(4)	1.536(6)
C13–C14	1.504(3)	1.511(4)	1.531(4)	1.513(7)
bond angles				
C13–N2–C15	116.8(2)	117.0(2)	119.2(2)	119.3(4)
N2–C13–C14	108.7(2)	108.8(2)	113.5(2)	114.4(4)
N2–C13–C12	111.9(2)	112.3(2)	112.0(2)	108.0(4)
C12–C13–C14	108.5(2)	109.8(2)	107.4(2)	109.2(4)
torsion angles				
C14–C13–N2–C15	–97.8(3)	–96.7(3)	–75.2(4)	–74.9(6)
C12–C13–N2–C15	142.4(2)	141.6(2)	163.0(2)	–163.3(5)
C11–C12–C13–N2	–79.0(2)	–81.9(3)	–71.6(3)	70.8(5)
C11–C12–C13–C14	161.1(2)	157.0(2)	163.1(2)	–164.2(4)
C13–N2–C15–C16	–68.3(3)	–69.1(3)	–94.3(3)	–99.2(6)
C13–N2–C15–C17	168.5(2)	165.7(3)	142.5(3)	138.7(7)
N1–C11–C12–C13	177.7(2)	113.2(2)	–173.6(2)	119.6(4)

1.469 \AA reported for secondary amines.^[27] Values are rather in the range expected for $\text{C}(\text{sp}^3)-\text{N}(\text{sp}^2)$ single bonds. In all of the four structures the amine hydrogen atom, experimentally located by Fourier methods, is displaced from the plane defined by N2 and the adjacent C13 and C15 atoms, showing a distorted sp^3 geometry of N2.

The local conformation of the common part of the four molecules is well described by the torsion angles around the five bonds $\text{C11}-\text{C12}$, $\text{C12}-\text{C13}$, $\text{C13}-\text{N2}$, $\text{N2}-\text{C15}$ and $\text{C15}-\text{C16}$ (see Table 4). The similarities among the four compounds are remarkable: indeed the conformational preferences towards *trans* or *gauche* arrangements of these dihedral angles are rather well defined and seem to be only marginally influenced by the presence of an intramolecular hydrogen bond, as found in **13**. Specifically, the torsion angle around $\text{C12}-\text{C13}$ is dictated by the expected preferential location of the CF_3 group, rather than N2, *trans* to C11. Similarly, in the case of the torsion angles around $\text{N2}-\text{C15}$, the “larger” sp^3 carbon C17, rather than the sp^2 C16, is arranged *trans* to the C13 atom, which has a bulky environment. The conformation around $\text{C13}-\text{N2}$ is more difficult to account for just considering local features. However, all of the four compounds display a conformation with the C12 nearly *trans* to C15, possibly due to cooperative conformational effects. Finally, the conformation around $\text{C11}-\text{C12}$ appears to favor a *transoid* arrangement (i.e., from *trans* to *skew*) of N1 with respect to C13, depending upon the nature of the groups bound to N1. The basic features of the turn-like structure are in essence related to the *gauche*, *trans*, *gauche* sequence of, respectively, the torsion angles $\text{C11}-\text{C12}-\text{C13}-\text{N2}$, $\text{C12}-\text{C13}-\text{N2}-\text{C15}$ and $\text{C13}-\text{N2}-\text{C15}-\text{C16}$, with *gauche* angles of the same sign. As readily observable in Figure 8, this property is common to all of the molecules discussed herein, with the notable exception of **9c**. In all of the four crystal structures, the local conformations discussed above seem to bring the stereoelectronically demanding CF_3 group in a stereochemically favorable environment. In the case of **3a**, **9a** and **13** this position is represented by the exterior surface of the turn: it is in this respect clear that the relative configuration of the CF_3 -

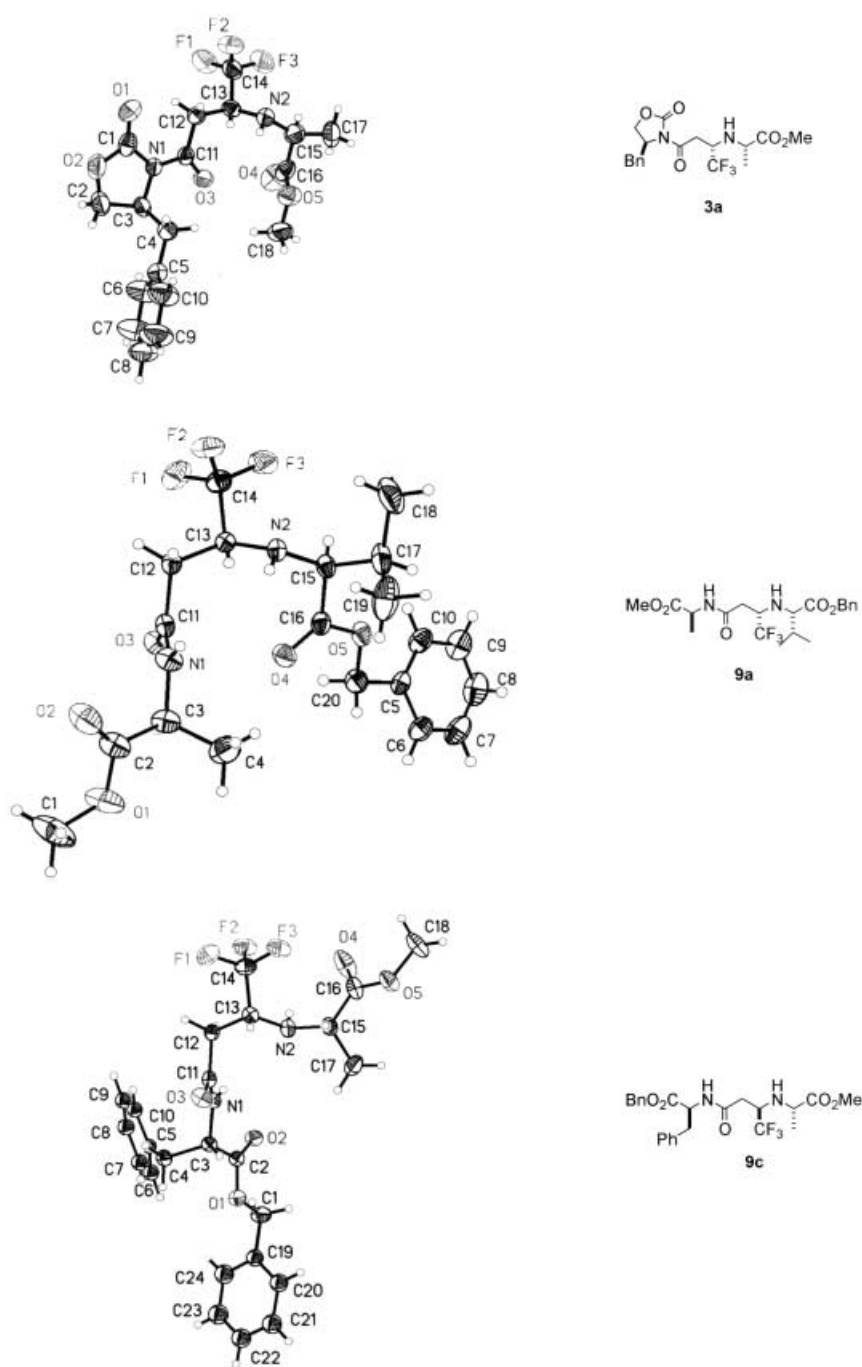


Figure 8. ORTEP drawings of **3a**, **9a** and **9c**.

bearing C13 atom and the C15 amino-acid center, which is identical in **3a**, **9a** and **13** and opposite in **9c**, has a key role in determining the stability of the turn-like conformation, whereas the absolute configurations of C13 and C15 fix the sign of the torsion angles around the adjacent C13–N2 and C13–C12 bonds, and thus the chirality of the turn. These findings are in agreement with the results obtained by ^1H NMR spectroscopy in solution on the hydroxamates **13** and **14**, and strongly suggest that a *syn* configuration of the $[-\text{CH}(\text{CF}_3)\text{NHCH}(\text{R})-]$ fragment is a fundamental requisite for the formation of a stable turn-like conformation. One can therefore say that, with the appropriate configuration, the

C13– CF_3 group behaves as a valid mimic of the retro-amide carbonyl group in Gellman's retropeptides.

In order to verify the respective influences of the neighboring CF_3 and of the substituents directly bonded to the NH group, a series of ab initio geometry optimization calculations was performed. For the sake of comparison, analogous calculations were carried out on the structure **TI** (Figure 9), which represents a mimic of the so called “tetrahedral intermediate” in the protease mediated hydrolysis reaction, on model $\psi[\text{NHCH}(\text{CF}_3)]$ -amides **15a–c** (Figure 9), and on $\psi[\text{NHCH}(\text{CF}_n\text{H}_{3-n})]$ structures ($n = 0–2$) **16–18**, which have lower degrees of fluorination (Figure 10). These calculations were accomplished in order to check and compare structural and electronic features of the tetrahedral intermediate **TI** and those of the fluorinated peptidomimetics **15–18**. Several studies have demonstrated that the “tetrahedral intermediate”, closely resembling (according to Hammond's postulate) the transition state leading to the hydrolysis of amides or esters, is characterized by the presence of a negatively charged oxygen atom bound to an sp^3 carbon, belonging to the scissile amide or ester group.^[28] Other studies on the mechanism of serine proteases in different conditions^[29] have shown that the tetrahedral intermediate is a

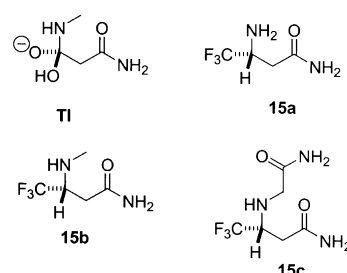


Figure 9. Calculated structures of model PMR $\psi[\text{NHCH}(\text{CF}_3)]$ Gly frameworks and tetrahedral hydrolysis intermediate **TI**.

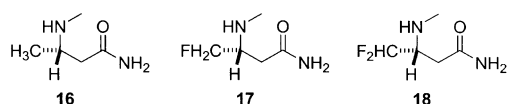


Figure 10. Calculated structures of model PMR ψ [NHCH(R_F)]Gly frameworks.

good model to explain reactivity and draw mechanistic conclusions.

Simplified models catching all the basic chemical and conformational features of the ψ [NHCH(CF_nH_{3-n})] systems and of **TI** were used in order to reduce the computation time and allow the use of a suitable level of theory in the QM ab initio calculations. Ab initio calculations were performed in the perspective of calculating and comparing the stereoelectronic features of our model compounds to those of **TI**, which is impossible to isolate and whose properties are not easily measurable. Moreover, using a high level of theory, trends in the related compounds examined can be evidenced with high accuracy.

The starting structure of each model peptide was built using the MacroModel package with a spatial disposition of the groups mimicking their respective disposition in the X-ray structure (see Supporting Information). Each structure was first minimized through a Molecular Mechanics approach using the Amber^[30] force field. As expected, the bond angle of the C_A-N_F-X (X = C_B, H_F) group covalently bound to the CF₃ moiety is far from 120°: this angle is actually close to 109.0° for each starting structure of the peptides studied.

In contrast, the structures obtained after the quantum mechanical level optimization (see Figure 11 and data reported in Table 5) clearly show that when a substituent (X = C_B) is present on the NH group a widening of the C_A-N_F-C_B angle to a value around 120° is observed, matching the experimentally determined X-ray structure. This underlines the importance of the correct theoretical treatment of this kind of peptide models.

The NH₂ group in **15a** is bound to a C_A-CF₃ system with no further ramification. This primary amine nitrogen displays the typical structural characteristics of an sp³ atom (Table 5). Increasing the degree of substitution on the amino group by the insertion of a CH₃ moiety (**15b**), determines dramatic effects on the bond angle on nitrogen. In fact, the C_A-N_F-C_B bond angle becomes clearly distorted. In the optimized structure it adopts a value of

Table 5. C_A-N_F-X bond angle and C_A-N_F bond length values for the optimized peptide structures.^[a]

Compound	C _A -N _F -X angle [°]	C _A -N _F -H _{F1} angle [°]	C _A -N _F bond length [Å]
15a (X = H _{F2})	112.625	112.877	1.44
15b (X = C _B)	120.791	109.501	1.45
15c (X = C _B)	120.526	111.057	1.45
16 (X = C _B)	118.679	108.300	1.47
17 (X = C _B)	119.896	108.624	1.45
18 (X = C _B)	120.791	109.501	1.45
TI	117.422	110.330	1.49

[a] Atom tags are defined in Figure 11.

120.8°, which could suggest an sp²-type geometry. However, the N_F-H bond does not lie in the same plane as the two carbons bound to the N_F atom, in agreement with the results of X-ray diffraction on the PMR peptides **3a**, **9a**, **9c** and **13**. Analysis of **15c**, obtained by substitution of one of the hydrogen atoms on the primary amino group of **15a** with -CH₂CONH₂, confirms the tendency of the substituted α-CF₃ amino group N_F to adopt a bond angle value around 120°, with an overall local geometry similar to that of **15b**, thus confirming the highly distorted sp³ geometry already evidenced for the N_F **15b**.

Three analogues of **15b**, namely **16–18** (see Figure 12), characterized by the different number of F atoms in the methyl group bound to the NH-substituted C_A atom, were studied next with the aim of gaining deeper insight into the

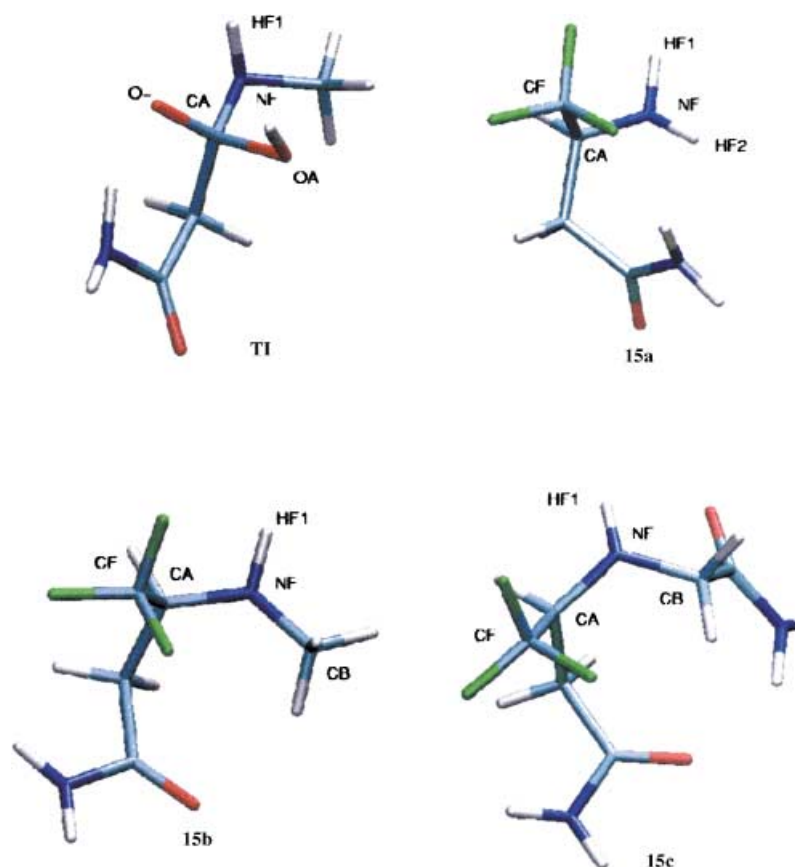


Figure 11. Optimized geometries for the structures for **TI**, and for the amides **15a–c**.

effect of increasing fluorine substitution on the geometry of NH. Inspection of Table 5 shows that the $C_A-N_F-C_B$ angle tends to assume a value closer to 120° as the fluorine atom number increases. This can be likely interpreted in terms of an increasing steric hindrance of the fluoromethyl group centered on C_F , which determines a progressive widening of the C_A-N-C_B angle, which is particularly distorted in the case of the bulky CF_3 group. This hypothesis is supported by analysis of the 203 crystal structures having secondary amine functions found in the CCD (see Supporting Information). It is indeed apparent that the largest C-NH-C bond angles are displayed by those compounds having sterically demanding substituents bound to the α -amino carbon. In order to completely rule out the possibility that factors other than steric hindrance are involved in the distortion of the $C_A-N_F-C_B$ angle, population analysis was run on the optimized structure. The results showed that, as expected, the C_A-N_F bond involving the amino group flanking the CF_3 substituent does not have any double bond character.

In the case of **TI** the analogous angle (defined by the tetrahedral carbon bearing two oxygen atoms, the NH group and the C_B attached to the N atom) displays a value of about 118.7° . This value is very close to the value of the angle $C_A-N_F-C_B$ calculated for the fluorinated peptidomimetics.

The stereoelectronic features of the three model CF_3 -amides **15a–c** were evaluated with the calculation of their molecular electrostatic potential (MEP); the surfaces of the amides are displayed in Figure 12. All the molecules display a high local concentration of negative charge on the CF_3 group,

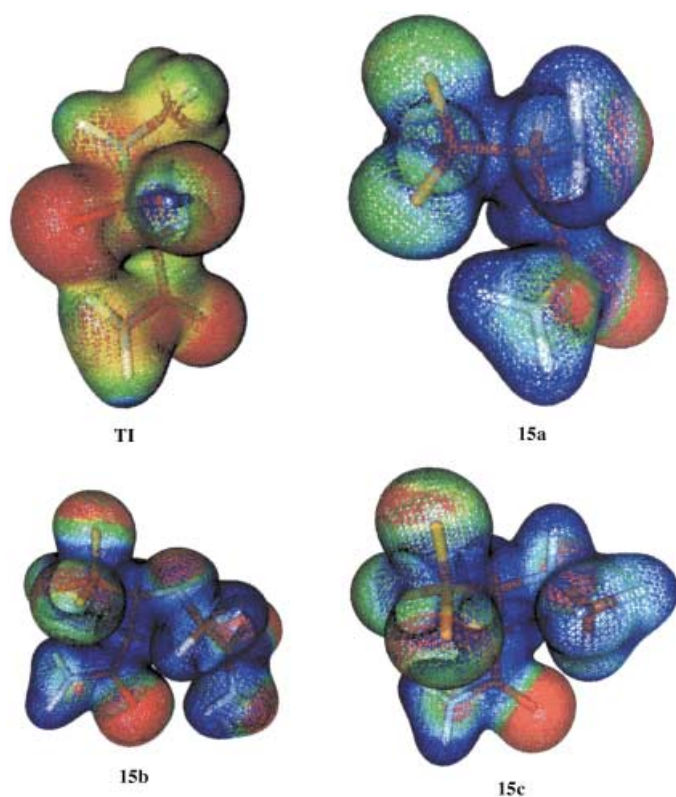


Figure 12. The molecular electrostatic potential surfaces (MEP) for the tetrahedral intermediate **TI**, and CF_3 -amides **15a–c**. The color code is from blue for positive potential to red for negative potential.

influencing the dipolar characteristics of each molecule. The concentration of negative charge is located in a position strictly correlated to the one of the negatively charged O atoms in molecule **TI**. The presence of a net negative charge on **TI** makes the overall MEP more negative. The absence of such a charge in the fluorine containing peptidomimetics favors the presence of positively or neutrally charged patches on the MEP surface.

The presence of such a localized negatively charged region can be extremely important, together with the peculiar geometrical aspects of the NH groups of these compounds, for the recognition of the designed peptides by putative receptors.

Conclusion

Conceptually new types of peptidomimetics, PMR and PMRI $\psi[NHCH(CF_3)]Gly$ peptides, are now available through the effective solution-phase chemistry described in this paper, as well as through solid-phase chemistry, as previously reported.^[7d] Several PMR $\psi[NHCH(CF_3)]Gly$ peptides investigated by X-ray diffraction show a remarkable proclivity to adopt turn-like conformations independent of the presence of $C=O \cdots H_b-N$ intramolecular hydrogen bonding, which was shown to be of paramount importance for stabilizing the turn-like conformations adopted by Gellman's unfluorinated retropeptides. This is clearly shown by the strong similarity in the values of the torsion angles defining the turns in the crystal structure of compounds **3a**, **9a**, and **13**, having the same *syn*-configuration at the C13 and C15 stereocenters, among which only **13** displays intramolecular hydrogen bonding. In contrast, no turn-like structure is displayed by **9c**, which has *anti*-configuration at the same centers. Similar turn-like conformational states were found to be highly populated in $CDCl_3$ solution for $\psi[NHCH(CF_3)]$ -PMR tripeptides **12** (which is an exact structural analogue of one of Gellman's retropeptides), **13** and **14**. These striking conformational features can be ascribed to the heavy stereoelectronic demands of the CF_3 group,^[31] and possibly to its preferential solvation once the turn-like conformation has been established. In fact, it is apparent that in such turn-like conformations the CF_3 group points towards the outside position of the turn itself, independent of the other substituent groups examined. These findings, which deserve further investigation, suggest that the CF_3 group itself might constitute an important stabilizing factor for the turn. This could represent a new general concept for the rational design of linear peptidomimetics incorporating a turn-like secondary structure. Finally, ab initio computational studies showed that the $[-CH(CF_3)NH-]$ group has very peculiar characteristics, which are intermediate between a peptide bond mimic and a proteolytic transition state analogue. We believe that $\psi[NHCH(CF_3)]$ PMR peptides hold the potential to become an important class of peptidomimetics in biomedical and pharmaceutical field.

Experimental Section

General details: THF was freshly distilled from Na; diisopropylamine was freshly distilled from CaH₂. In all other cases, commercially available reagent-grade solvents were employed without purification. All reactions where an organic solvent was employed were performed under nitrogen atmosphere, after flame-drying of the glass apparatus. Melting points (m.p.) are uncorrected and were obtained on a capillary apparatus. TLC were run on silica gel 60 F₂₅₄ Merck. Flash chromatographies (FC) were performed with silica gel 60 (60–200 μm, Merck). ¹H NMR spectra were run at 250, 400 or 500 MHz. Chemical shifts are expressed in ppm (δ), using tetramethylsilane (TMS) as internal standard for ¹H and ¹³C nuclei (δ_H and δ_C = 0.00), while C₆F₆ was used as external standard (δ_F 162.90) for ¹⁹F.

Experimental for the aza-Michael reaction: Synthesis of **3c** is described as an example. To a stirred solution of (*E,S*)-**2a**^[9] (80 mg, 0.27 mmol) and **L-1b** (131 mg, 0.54 mmol) in dry CH₂Cl₂ (3.4 mL) was added neat *sym*-collidine (0.14 mL, 1.08 mmol). After 64 h at RT the solvent was removed in vacuo, the crude dissolved in EtOAc and washed once with a 1N HCl. The organic layer was dried over anhydrous Na₂SO₄, filtered, the solvent removed in vacuo, and the crude purified by FC (hexane/diethyl ether 65:35) affording diastereoisomerically pure **3c** (116 mg, 78.5%) and its minor diastereoisomer **4c** (20 mg, 13.5%). **3c**: *R*_f = 0.21 (hexane/EtOAc 80:20); [α]_D²⁵ = +28.3° (*c* = 1.0, CHCl₃); m.p. 102–103 °C; FTIR (film): $\tilde{\nu}_{\text{max}}$ = 3449, 1794, 1700, 1385, 1258, 1120 cm⁻¹; ¹H NMR (250 MHz, CDCl₃): δ = 7.38–7.20 (m, 10H), 5.13 (d, *J* = 12.1 Hz, 1H), 5.06 (d, *J* = 12.1 Hz, 1H), 4.70 (m, 1H), 4.24 (m, 1H), 4.16 (dd, *J* = 8.8, 2.8 Hz, 1H), 3.62 (m, 1H), 3.42 (dd, *J* = 15.3, 3.6 Hz, 1H), 3.36 (m, 2H), 3.15 (dd, *J* = 15.3, 9.6 Hz, 1H), 2.77 (dd, *J* = 13.7, 10.1 Hz, 1H), 2.01 (m, 1H), 1.88 (brs, 1H), 0.96 (d, *J* = 6.7 Hz, 3H), 0.85 (d, *J* = 6.7 Hz, 3H); ¹⁹F NMR (250 MHz, CDCl₃): δ = –77.5 (d, *J* = 6.7 Hz); ¹³C (250 MHz, CDCl₃): δ = 174.8, 169.3, 153.6, 135.6, 135.4, 129.4, 129.0, 128.6, 128.4, 128.2, 127.4, 126.0 (q, *J* = 282.3 Hz), 66.8, 66.6, 66.5, 55.7 (q, *J* = 29.3 Hz), 55.5, 37.9, 36.3, 31.8, 19.3, 17.5; MS (70 eV): *m/z* (%): 507 (8) [*M*⁺+H], 371 (90), 91 (100).

4c: *R*_f = 0.17 (hexane/EtOAc 80:20); ¹⁹F NMR (250 MHz, CDCl₃): δ = –77.1 (d, *J* = 7.2 Hz).

Typical procedure synthesis of the PMR peptides: A 30% aqueous H₂O₂ solution (0.86 mL, 0.85 mmol) followed by solid LiOH (5 mg, 0.21 mmol) was added to a cooled solution of **3c** (97 mg, 0.21 mmol) in THF/H₂O 4:1 (1.5 mL) at 0 °C and under nitrogen atmosphere. After 60 min the reaction was quenched with saturated aqueous Na₂SO₃, warmed to rt, and extracted three times with AcOEt, and the combined organic layers were dried over anhydrous Na₂SO₄, filtered, and concentrated in vacuo. Purification by FC (hexane/AcOEt 1:1 until complete recovery of the oxazolidin-2-one and then MeOH) afforded the acid (50 mg, 68%). To a stirred mixture of this acid (30 mg, 0.08 mmol) and **L-1a** (12 mg, 0.08 mmol) in dry DMF (1 mL) was added, at 0 °C under nitrogen atmosphere, neat *sym*-collidine (0.032 mL, 0.85 mmol), followed by solid HOAt (11 mg, 0.08 mmol) and solid HATU (31 mg, 0.08 mmol). After 40 min the solution was quenched with 1N HCl, warmed to RT, and extracted with AcOEt, and the combined organic layers dried over anhydrous Na₂SO₄, filtered, and concentrated in vacuo. Purification by FC (hexane/AcOEt 75:25) afforded **9a** (35 mg, quant). *R*_f = 0.34 (hexane/EtOAc 70:30); [α]_D²⁵ = –9.2° (*c* = 0.9, CHCl₃); m.p. 70–71 °C; FTIR (KBr): $\tilde{\nu}_{\text{max}}$ = 3324, 1745, 1647, 1152 cm⁻¹; ¹H NMR (250 MHz, CDCl₃): δ = 7.42–7.32 (m, 5H), 7.10 (br d, *J* = 6.2 Hz, 1H), 5.20 (d, *J* = 12.0 Hz, 1H), 5.11 (d, *J* = 12.0 Hz, 1H), 4.59 (m, 1H), 3.74 (s, 3H), 3.55 (m, 1H), 3.46 (d, *J* = 5.0 Hz, 1H), 2.65 (dd, *J* = 15.4, 3.1 Hz, 1H), 2.43 (dd, *J* = 15.4, 9.3 Hz, 1H), 2.00 (m, 2H), 1.44 (d, *J* = 6.9 Hz, 3H), 0.96 (d, *J* = 6.6 Hz, 3H), 0.88 (d, *J* = 6.6 Hz, 3H); ¹⁹F NMR (250 MHz, CDCl₃): δ = –73.6 (d, *J* = 6.9 Hz); ¹³C (250 MHz, CDCl₃): δ = 174.4, 173.5, 168.2, 135.5, 128.6, 128.4, 126.0 (q, *J* = 283.0 Hz), 66.9, 65.5, 56.0 (q, *J* = 29.6 Hz), 52.4, 48.3, 36.1, 31.9, 19.0, 18.0, 17.6; MS (70 eV): *m/z* (%): 433 (3) [*M*⁺+H], 297 (100), 91 (100).

NMR studies on the secondary structure of ψ[NHCH(CF₃)]-PMR peptides: ¹H NMR spectra were measured in CDCl₃ with a 600 MHz spectrometer. The concentrations of the samples were 3, 0.7 and 0.04 mM with temperatures ranging from 293 to 213 K. Chemical shifts are given in δ and referred to the CDCl₃ used as the solvent. 2D ROESY spectra were acquired in the phase sensitive TPPI mode, with 2 k × 512 complex FIDs, spectral width of 9615 Hz, recycling delay 1.6 s, 56 scans, at 213 and 293 K with mixing times of 300 ms. The spectra were transformed and weighted

with a 90° shifted sine-bell squared function to 1 k × 1 k real data points.

Molecular modelling on 13: Molecular models were build using a Silicon Graphics 4D35GT workstation running the Insight II & Discover software. Molecular mechanics (MM) and molecular dynamics (MD) were carried out using CVFF as force field. The starting geometry of the compounds were generated using standard bond lengths and angles. The models were then energy minimised without NOE constraints, using a optimised cycle until a maximum energy derivative of 4.18 × 10⁻² kJ mol⁻¹ Å⁻¹ was reached. The subsequent unrestrained molecular dynamics calculation, performed for 100 ps at 1000 K temperature and sampling the trajectory every 1 ps, followed by minimisation, led to different structures.

X-ray structure analysis of 3a: Colorless lath of 0.45 × 0.10 × 0.05 mm size, orthorhombic *P*₂₁₂₁, *a* = 5.2797(4), *b* = 13.3423(9), *c* = 27.2759(18) Å, *V* = 1921.4(2) Å³, *Z* = 4, ρ_{calcd} = 1.391 g cm⁻³, 2θ_{max} = 61°, diffractometer Siemens Smart CCD, MoK_α (λ = 0.71073 Å), ω scan, *T* = 293(2) K, 15 758 reflections collected of which 5668 were independent (*R*_{int} = 0.0643), direct primary solution and refinement on *F*²,^[32] 256 refined parameters, amino hydrogen atom located in a difference Fourier synthesis and refined with restrained N–H bond length, other hydrogen atoms riding, *R*1 [*I* > 2σ(*I*)] = 0.0471, *wR*² (all data) = 0.1123, residual electron density 0.168 (–0.149) e Å⁻³, absolute structure could not be determined.

X-ray structure analysis of 9a: Needle colorless crystal with dimension of 0.15 × 0.2 × 0.8 mm, orthorhombic *P*₂₁₂₁, *a* = 9.106(5), *b* = 15.611(5), *c* = 16.770(5) Å, *V* = 1383(1) Å³, *Z* = 4, ρ_{calcd} = 1.205 g cm⁻³, μ = 0.868 mm⁻¹, Siemens P4 diffractometer with graphite monochromated CuK_α radiation (λ = 1.54179 Å), θ/2θ scan technique, room temperature, a total of 3055 reflections (2862 unique, *R*_{int} = 0.016) collected up to 136° in 2θ. Structure solved by direct methods^[33] and refined on *F*²,^[32] amino hydrogen freely refined, other hydrogen atoms riding, *R*1 = 0.0397 (*R*_w = 0.100) for 2283 observed reflections [*I* ≥ 2σ(*I*)] and 280 parameters refined, and *R*1 = 0.0517 (*R*_w = 0.131) for all data, residual electron density of 0.126 and –0.104 e Å⁻³.

X-ray structure analysis of compound 9c: Needle colorless crystal with dimension of 0.2 × 0.3 × 0.8 mm, hexagonal *R*3, *a* = 35.624(5), *c* = 5.210(5) Å, *V* = 5726(6) Å³, *Z* = 9, ρ_{calcd} = 1.254 g cm⁻³, μ = 0.870 mm⁻¹, Siemens P4 diffractometer with graphite monochromated CuK_α radiation (λ = 1.54179 Å), θ/2θ scan technique, room temperature, a total of 2644 reflections (2435 unique, *R*_{int} = 0.019) collected up to 130° in 2θ. Structure solved by direct methods^[33] and refined on *F*²,^[32] amino hydrogen freely refined, other hydrogen atoms riding, *R*1 = 0.0493 (*R*_w = 0.126) for 2122 observed reflections [*I* ≥ 2σ(*I*)] and 256 parameters refined, and *R*1 = 0.0575 (*R*_w = 0.134) for all data, residual electron density of 0.286 and –0.169 e Å⁻³.

Ab initio calculations: All ab initio calculations were carried out using the Gaussian 98^[34] molecular orbital package on an Origin 200 Silicon Graphics workstation. The initial geometry of each model peptide was chosen to mimic the situation in the experimentally determined crystal structure (see Tables 4 and 5, and Supporting Information). Initial geometries were built using the Macromodel6.5 package.^[35] Three model peptides were chosen with different substitutions on the NH (labeled N_F in Figure 11) group bound to the CF₃ carrying carbon atom. Structure **15a** is characterized by the presence of a CF₃-CH-NH₂ group, structure **15b** by the presence of a CF₃-CH-NH-CH₃ while structure **15c** carries a CF₃-CH-NH-CH₂-CO-NH₂. These groups were chosen to mimic different steric and electronic features of each peptide. The geometries were optimized at DFT level^[36] using the B3LYP^[37] functional and the 6-311++G** basis. The DFT B3LYP level of theory is known to give very accurate energy values, and the use of a basis set like 6-311++G** guarantees that possible polarization effects due to the presence of the fluorine atoms are taken into account.^[38] Previous calculations on peptide models using this approach have proved to yield results in terms of peptide geometry which are comparable to those obtained using much higher levels of theory. Population analysis was run on the minimized structures at the RHF 6-31G** level.

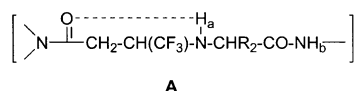
Acknowledgement

We thank the European Commission (IHP Network grant “FLUOR MMPI” HPRN-CT-2002-00181), MIUR (Cofin 2002, Project “Peptidi

Sintetici Bioattivi”) and CNR for financial support. Politecnico di Milano is gratefully acknowledged for fellowships to A.V. and F.B.

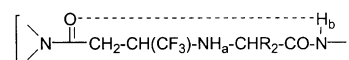
- [1] A. Loffet, *J. Pept. Sci.* **2002**, *8*, 1–7.
- [2] a) G. L. Olson, D. R. Bolin, M. P. Bonner, M. Bös, C. M. Cook, D. C. Fry, B. J. Graves, M. Hatada, D. E. Hill, M. Kahn, V. S. Madison, V. K. Rusiecki, R. Sarabu, J. Sepinwall, G. P. Vincent, M. E. Voss, *J. Med. Chem.* **1993**, *36*, 3039–3049; b) J. Gante, *Angew. Chem.* **1994**, *106*, 1780–1802; *Angew. Chem. Int. Ed. Engl.* **1994**, *33*, 1699–1720; c) D. Leung, G. Abbenante, D. P. Fairlie, *J. Med. Chem.* **2000**, *43*, 305–341.
- [3] a) M. Goodman, M. Chorev, *Acc. Chem. Res.* **1979**, *12*, 1–7; b) M. Chorev, C. G. Willson, M. Goodman, *J. Am. Chem. Soc.* **1977**, *99*, 8075–8076; c) M. Chorev, M. Goodman, *Acc. Chem. Res.* **1993**, *26*, 266–273; d) M. Chorev, M. Goodman, *Trends Biotechnol.* **1995**, *13*, 438–445; e) M. D. Fletcher, M. M. Campbell, *Chem. Rev.* **1998**, *98*, 763–795. The idea of retropeptides originates from the fact that peptides and proteins, like other biopolymers, have a direction and therefore are inherently non-palindromic. The sense of direction conventionally proceeds from the amino terminus (which is written on the left, see Figure 1) to the carboxy terminus (written on the right).
- [4] The retro- and retro-inverso peptide concepts are finding increasing applications in medicinal chemistry. For some examples: a) J. Wermuth, S. L. Goodman, A. Jonczyk, H. Kessler, *J. Am. Chem. Soc.* **1997**, *119*, 1328–1335; b) A. Phan-Chan Du, M. C. Petit, G. Guichard, J. P. Briand, S. Muller, M. T. Cung, *Biochemistry* **2001**, *40*, 5720–5727; c) N. Nishikawa, H. Komazawa, A. Orikasa, M. Yoshikane, J. Yamaguchi, M. Kojima, M. Ono, I. Itoh, I. Azuma, H. Fujii, J. Murata, I. Saiki, *Bioorg. Med. Chem. Lett.* **1996**, *6*, 2725–2728; d) H. Fujii, N. Nishikawa, H. Komazawa, A. Orikasa, M. Ono, I. Itoh, J. Murata, I. Azuma, I. Saiki, *Oncol. Res.* **1996**, *8*, 333–342; e) G. Guichard, F. Connan, R. Graff, M. Ostantkovich, S. Muller, J.-G. Guillet, J. Choppin, J.-P. Briand, *J. Med. Chem.* **1996**, *39*, 2030–2039; f) P. Juvvadi, S. Vunnam, R. B. Merrifield, *J. Am. Chem. Soc.* **1996**, *118*, 8989–8997; g) K. Witte, J. Skolnick, C. H. Wong, *J. Am. Chem. Soc.* **1998**, *120*, 13042–13045; h) F. Nargi, E. Kramer, J. Mezencio, J. Zamparo, C. Whetstone, M. H. V. Van Regenmortel, J. P. Briand, S. Muller, F. Brown, *Vaccine* **1999**, *17*, 2888–2893; i) L. K. Iwai, M. A. Duranti, L. C. J. Abel, M. A. Juliano, J. Kalil, L. Juliano, E. Cunha-Neto, *Peptides* **2001**, *22*, 853–860; j) A. Verdoliva, M. Ruvo, M. Villain, G. Cassani, G. Fassina, *Biochim. Biophys. Acta* **1995**, *1253*, 57–62; k) U. Wenzel, K. Jouvenal, D. Tripier, K. Ziegler, *Biochem. Pharmacol.* **1995**, *49*, 479–487; l) M. A. Bednarek, M. V. Silva, B. Arison, T. MacNeil, R. N. Kalyani, R.-R. C. Huang, D. H. Weinberg, *Peptides* **1999**, *20*, 401–409; m) N. Beglova, S. Maliartchouk, I. Ekiel, M. C. Zaccaro, H. U. Saragovi, K. Gehring, *J. Med. Chem.* **2000**, *43*, 3530–3540; n) A. Carotti, A. Carrieri, S. Cellamare, F. P. Fanizzi, E. Gavuzzo, F. Mazza, *Biopolymers Pept. Sci.* **2001**, *60*, 322–332; o) T. Haack, Y. M. Sanchez, M.-J. Gonzalez, E. Giral, *J. Pept. Sci.* **1997**, *3*, 299–313; p) M. Goodman, R.-H. Mattern, P. Gantzel, A. Santini, R. Iacovino, M. Saviano, E. Benedetti, *J. Pept. Sci.* **1998**, *4*, 229–238; q) D. Seebach, M. Rueping, P. I. Arvidsson, T. Kimmerlin, P. Micuch, C. Noti, D. Langenegger, D. Hoyer, *Helv. Chim. Acta* **2001**, *84*, 3503–3510; r) M. Marino, A. Ippolito, G. Fassina, *Eur. J. Immunol.* **1999**, *29*, 2560–2566; s) J. A. Carver, G. Esposito, P. Viglino, F. Fogolari, G. Guichard, J.-P. Briand, M. H. V. Van Regenmortel, F. Brown, P. Mascagni, *Biopolymers* **1997**, *41*, 569–590; t) J. F. Hernandez, J. M. Soleilhac, B. P. Roques, M. C. Fournié-Zaluski, *J. Med. Chem.* **1988**, *31*, 1825–1831; u) S. L. Roderick, M. C. Fournié-Zaluski, B. P. Roques, B. W. Matthews, *Biochemistry* **1989**, *28*, 1493–1497.
- [5] For a preliminary communication on the synthesis of PMR and PMRI ψ [NHCH(CF₃)]Gly peptides: a) A. Volonterio, P. Bravo, M. Zanda, *Org. Lett.* **2000**, *2*, 1827–1830; a conceptually related peptide bond surrogate ψ [CH(CN)NH] has been reported: b) S. Herrero, M. L. Suárez-Gea, R. González-Muñiz, M. T. García-López, R. Herranz, S. Ballaz, A. Barber, A. Fortuño, J. Del Río, *Bioorg. Med. Chem. Lett.* **1997**, *7*, 855–860; for some recent examples of fluorine containing peptidomimetics: c) G. S. Garrett, S. J. McPhail, K. Tornheim, P. E. Correa, J. M. McIver, *Bioorg. Med. Chem. Lett.* **1999**, *9*, 301–306; d) M.-A. Poupard, G. Fazal, S. Goulet, L.-T. Mar, *J. Org. Chem.* **1999**, *64*, 1356–1361; e) M. Eda, A. Ashimori, F. Akahoshi, T. Yoshimura, Y. Inoue, C. Fukaya, M. Nakajima, H. Fukuyama, T. Imada, N. Nakamura, *Bioorg. Med. Chem. Lett.* **1998**, *8*, 919–924 and references therein; f) R. V. Hoffman, J. Tao, *Tetrahedron Lett.* **1998**, *39*, 4195–4198; g) P. A. Bartlett, A. Otake, *J. Org. Chem.* **1995**, *60*, 3107–3111; h) L. G. Boros, B. Decorte, R. H. Gimi, J. T. Welch, Y. Wu, R. E. Handschumacher, *Tetrahedron Lett.* **1994**, *35*, 6033–6036; i) L. Revesz, C. Briswalter, R. Heng, A. Leutwiler, R. Mueller, H.-J. Wuethrich, *Tetrahedron Lett.* **1994**, *35*, 9693–9696; j) R. P. Robinson, K. M. Donahue, *J. Org. Chem.* **1992**, *57*, 7309–7314; k) B. Bilgicer, A. Fichera, K. Kumar, *J. Am. Chem. Soc.* **2001**, *123*, 4393–4399; l) Y. Tang, G. Ghirlanda, N. Vaidehi, J. Kua, D. T. Mainz, W. A. Goddard, W. F. DeGrado, D. A. Tirrell, *Biochemistry* **2001**, *40*, 2790–2796; m) F. Bordusa, C. Dahl, H.-D. Jakubke, K. Burger, B. Koksche, *Tetrahedron: Asymmetry* **1999**, *10*, 307–313.
- [6] For clarity, throughout the paper we refer to the title compounds only as PMR and PMRI ψ [NHCH(CF₃)]Gly peptides. However ψ [NHCH(CF₃)] and ψ [CH(CF₃)NH] derivatives such as, HO-AA¹-[CH(CF₃)CH(R)C(O)]-AA²-OH and HO-AA¹-[C(O)CH(R)-CH(CF₃)]-AA²-OH, respectively, constitute two completely different classes of compounds, not related by any symmetry operation, when AA¹ ≠ AA². It is convenient to distinguish between the two forms when they are referred to a parent peptide such as H-AA¹-AA^R-AA²-OH.
- [7] Small libraries of PMR and PMRI ψ [NHCH(CF₃)]Gly peptides, as well as peptidyl hydroxamates having moderate inhibitory activity against MMP-9 (gelatinase B), have been already prepared through solid-phase synthesis: a) A. Volonterio, P. Bravo, N. Moussier, Zanda, M. *Tetrahedron Lett.* **2000**, *41*, 6517–6521; b) A. Volonterio, P. Bravo, M. Zanda, *Tetrahedron Lett.* **2001**, *42*, 3141–3144; c) A. Volonterio, S. Bellosta, P. Bravo, M. Canavesi, E. Corradi, S. V. Meille, M. Monetti, N. Moussier, M. Zanda, *Eur. J. Org. Chem.* **2002**, 428–438; d) M. Sani, P. Bravo, A. Volonterio, M. Zanda, *Collect. Czech. Chem. Commun.* **2002**, *67*, 1305–1319; for a recent paper on a novel class of retropeptides incorporating a stereodefined 3,3,3-trifluoroalanine mimic: e) M. Sani, L. Bruché, G. Chiva, S. Fustero, J. Piera, A. Volonterio, M. Zanda, *Angew. Chem.* **2003**, *115*, 2106–2109; *Angew. Chem. Int. Ed.* **2003**, *42*, 2060–2063.
- [8] See for example: L. R. Scolnick, A. M. Clements, J. Liao, L. Crenshaw, M. Hellberg, J. May, T. R. Dean, D. W. Christianson, *J. Am. Chem. Soc.* **1997**, *119*, 850–851.
- [9] a) A. Shibuya, M. Kurishita, C. Ago, T. Taguchi, *Tetrahedron* **1996**, *52*, 271–278; see also: b) T. Yamazaki, N. Shinohara, T. Kitazume, S. Sato, *J. Fluorine Chem.* **1999**, *97*, 91–96.
- [10] a) H. Urbach, R. Henning, *Tetrahedron Lett.* **1984**, *25*, 1143–1146; b) H. G. Eckert, M. J. Badian, D. Gantz, H.-M. Kellner, M. Volz, *Arzneim. Forsch.* **1984**, *34*, 1435–1447. The extraordinary efficiency and mildness of this aza-Michael reaction are due to the significantly greater reactivity of **2** with respect to other crotonates, which in turn is due to the concomitant presence of the electron-withdrawing CF₃ group and imide function. For other aza-Michael reactions with 4-substituted acceptors see: c) A. J. Burke, S. G. Davies, C. J. R. Hedgcock, *Synlett* **1996**, 621–622; d) J. d’Angelo, J. Maddaluno, *J. Am. Chem. Soc.* **1986**, *108*, 8112–8114; e) G. Cardillo, E. Di Martino, L. Gentilucci, C. Tomasini, L. Tomasoni, *Tetrahedron: Asymmetry* **1995**, *6*, 1957–1963; f) R. Amoroso, G. Cardillo, P. Sabatino, C. Tomasini, A. Trerè, *J. Org. Chem.* **1993**, *58*, 5615–5619; g) S. W. Baldwin, J. Aubé, *Tetrahedron Lett.* **1987**, *28*, 179–182; h) M. Hiram, T. Shigemoto, Y. Yamazaki, S. Ito, *J. Am. Chem. Soc.* **1985**, *107*, 1797–1798; i) M. E. Bunnage, S. G. Davies, C. J. Goodwin, I. A. S. Walters, *Tetrahedron: Asymmetry* **1994**, *5*, 35–36; j) S. G. Davies, I. A. S. Walters, *J. Chem. Soc. Perkin Trans. 1* **1994**, 1129–1139; k) S. G. Davies, O. Ichihara, I. A. S. Walters, *J. Chem. Soc. Perkin Trans. 1* **1994**, 1141–1147; l) J. M. Hawkins, T. A. Lewis, *J. Org. Chem.* **1994**, *59*, 649–652; m) N. Asao, T. Shimada, T. Sudo, N. Tsukada, K. Yazawa, Y. S. Gyoung, T. Ueyehara, Y. Yamamoto, *J. Org. Chem.* **1997**, *62*, 6274–6282; n) K. Rudolf, J. M. Hawkins, R. J. Loncharich, K. N. Houk, *J. Org. Chem.* **1988**, *53*, 3879–3882; o) J. M. Hawkins, G. C. Fu, *J. Org. Chem.* **1986**, *51*, 2820–2822; p) L. S. Liebeskind, M. E. Welker, *Tetrahedron Lett.* **1985**, *26*, 3079–3082; q) A. De, P. Basak, J. Iqbal, *Tetrahedron Lett.* **1997**, *38*, 8383–8386; r) Y. Yamamoto, N. Asao, T. Ueyehara, *J. Am. Chem. Soc.* **1992**, *114*, 5427–5429; s) F. Dumas, B. Mezhrab, J. d’Angelo, C. Riche, A. Chiaroni, *J. Org. Chem.* **1996**, *61*,

- 2293–2304; t) J. d'Angelo, J. Maddaluno, *J. Am. Chem. Soc.* **1986**, *108*, 8112–8114; u) B. Mezrhab, F. Dumas, J. d'Angelo, C. Riche, *J. Org. Chem.* **1994**, *59*, 500–503; v) G. Cardillo, S. Casolari, L. Gentilucci, C. Tomasini, *Angew. Chem.* **1996**, *108*, 1939–1941; *Angew. Chem. Int. Ed. Engl.* **1996**, *35*, 1848–1849; w) M. P. Sibi, U. Gorikunti, M. Liu, *Tetrahedron* **2002**, *58*, 8357–8363; x) S. Kobayashi, K. Kakumoto, M. Sugiura, *Org. Lett.* **2002**, *4*, 1319–1322; y) K. Drandarov, M. Hesse, *Tetrahedron Lett.* **2002**, *43*, 7213–7216; for a recent review: z) M. Liu, M. Sibi, *Tetrahedron* **2002**, *58*, 7991–8035.
- [11] Diastereomerically pure **3** were smoothly isolated by flash chromatography on silica gel.
- [12] The stereochemistry of **3a** was assigned by X-ray diffraction (see the Section on “Secondary structure of PMR ψ [NHCH(CF₃)]Gly peptide”), while the stereochemistry of the other major diastereomers **3b–j** was assigned on the basis of their spectral and chemical-physical similarities with **3a**. The stereochemistry of **5a**, major diastereomer derived from D-Ala-OMe **1a**, was determined by chemical correlation with **3a** after cleavage of the oxazolidinone auxiliary.
- [13] a) D. A. Evans, K. T. Chapman, J. Bisaha, *J. Am. Chem. Soc.* **1988**, *110*, 1238–1256; b) D. A. Evans, T. C. Britton, J. A. Ellman, R. L. Dorow, *J. Am. Chem. Soc.* **1990**, *112*, 4011–4030; see also: c) V. A. Soloshonok, C. Cai, V. J. Hruby, *Org. Lett.* **2000**, *2*, 747–750.
- [14] For a recent successful example of use of Sc(OTf)₃ in related reactions: C. L. Mero, N. A. Porter, *J. Org. Chem.* **2000**, *65*, 775–781.
- [15] D. A. Evans, T. C. Britton, J. A. Ellman, R. L. Dorow, *J. Am. Chem. Soc.* **1990**, *112*, 4011–4030. Oxazolidin-2-one auxiliaries were usually recovered in nearly quantitative yields after cleavage.
- [16] Only proline derived pseudo-tripeptide **9d**, obtained as a ca. 3:1 mixture of isomers at the peptide bond, and tetrapeptide **10** were isolated as foams.
- [17] It can be roughly estimated that the pK_b of the [NHCH(CF₃)] group should be 5 units lower than that of the parent unfluorinated group [NHCH(CH₃)]: a) R. E. Banks, J. C. Tatlow, B. E. Smart, *Organofluorine Chemistry: Principles and Commercial Applications*, Plenum Press, New York, **1994**, pp. 68–69; see also: b) N. Sewald, K. Burger, in *Fluorine-containing Amino Acids: Synthesis and Properties* (Eds.: V. P. Kukhar, V. A. Soloshonok), Wiley, Chichester, **1995**, pp. 139–220.
- [18] A. J. Souers, J. A. Ellman, *Tetrahedron* **2001**, *57*, 7431–7448 and references therein.
- [19] a) S. H. Gellman, B. R. Adams, G. P. Dado, *J. Am. Chem. Soc.* **1990**, *112*, 460–461; b) G. P. Dado, J. M. Desper, S. H. Gellman, *J. Am. Chem. Soc.* **1990**, *112*, 8630–8632; c) S. H. Gellman, G. P. Dado, G.-B. Liang, B. R. Adams, *J. Am. Chem. Soc.* **1991**, *113*, 1164–1173; d) G.-B. Liang, G. P. Dado, S. H. Gellman, *J. Am. Chem. Soc.* **1991**, *113*, 3994–3995; e) G. P. Dado, J. M. Desper, S. K. Holmgren, C. J. Rito, S. H. Gellman, *J. Am. Chem. Soc.* **1992**, *114*, 4834–4843; f) G. P. Dado, S. H. Gellman, *J. Am. Chem. Soc.* **1993**, *115*, 4228–4245; g) J. J. Novoa, M.-H. Whangbo, *J. Am. Chem. Soc.* **1991**, *113*, 9017–9026; h) J. Puiggali, J. A. Subirana, *Biopolymers* **1998**, *45*, 149–155.
- [20] a) H. Kessler, *Angew. Chem.* **1982**, *94*, 509–520; *Angew. Chem. Int. Ed.* **1982**, *512*–523.
- [21] These compounds were obtained as described in ref. [7c].
- [22] It is worth noting that the temperature dependence of the NH_b chemical shifts of epimers **13** and **14** seems to be convergent at higher temperature, which is more than reasonable for two closely similar structures.
- [23] We did not find any experimental evidence for intramolecular hydrogen bonds involving NH_a, despite the fact that it could form a six-membered ring **A**. One possible reason is that NH_a is a worse hydrogen-bond donor, since it is less acidic than NH_b.

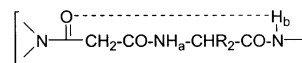


- [24] Also, for **14** free MD calculations were performed and, after minimization without constraints, many different structures were obtained.

- [25] CCDC-204501–204503 (**3a**, **9a** and **9c**) contain the supplementary crystallographic data for this paper. These data can be obtained free of charge via www.ccdc.cam.ac.uk/conts/retrieving.html (or from the Cambridge Crystallographic Data Centre, 12 Union Road, Cambridge CB2 1EZ, UK; fax: (+44)1223-336-033; or e-mail: deposit@ccdc.cam.ac.uk).
- [26] a) F. H. Allen, O. Kennard, *Chem. Des. Autom. News. Soc.* **1993**, 31–39; b) the results of the search for secondary amine structures R-NH-R¹ are elaborated in the Supporting Information. Among them, 29 structures (including **13**) with a RR¹CH-NH-CHR²R³, such as **3a**, **9a**, and **9c**, were found. The C-N-C angles of these structures span from 111.94 to 119.93°, therefore the values for PMR ψ [NHCH(CF₃)]Gly peptides fall within this range, although they are quite large and shifted toward the upper limit value; c) it is not surprising at all that **3a**, **9a** and **9c** do not display CO...NH intramolecular hydrogen bonds, which in contrast are present both in Gellman's retropeptides and in **13**. In fact, none of these PMR ψ [NHCH(CF₃)]Gly peptides incorporate a framework **B**, mimic of the Gellman's retropeptide unit **C** (see ref. [19]). This is likely due to the fact that amide and imide carbonyls are much better hydrogen-bond acceptors than carbonyls belonging to ester functions.



B



C

- [27] F. H. Allen, O. Kennard, D. G. Watson, L. Brammer, A. G. Orpen, R. Taylor, *J. Chem. Soc. Perkin Trans. 2* **1987**, S1–19.
- [28] a) S. Schroder, V. Daggett, P. A. Kollman, *J. Am. Chem. Soc.* **1991**, *113*, 8922–8925; b) V. Daggett, S. Schroder, P. A. Kollman, *J. Am. Chem. Soc.* **1991**, *113*, 8926–8935.
- [29] G. Colombo, S. Toba, K. M. Merz, Jr., *J. Am. Chem. Soc.* **1999**, *121*, 3486–3493.
- [30] D. Q. McDonald, W. C. Still, *J. Am. Chem. Soc.* **1996**, *118*, 2073–2077.
- [31] See ref. [17], pp. 537–538.
- [32] G. M. Sheldrick, SHELXL97, Release 97-2, Program for the Refinement of Crystal Structures, University of Göttingen, Göttingen (Germany), **1997**.
- [33] A. Altomare, M. C. Burla, M. Camalli, G. L. Cascarano, C. Giacovazzo, A. Guagliardi, A. G. G. Molteni, G. P. Polidori, R. Spagna, *J. Appl. Crystallogr.* **1999**, *32*, 115–119.
- [34] *Gaussian 98 (Revision A.9)*, M. J. Frisch, G. W. Trucks, H. B. Schlegel, G. E. Scuseria, M. A. Robb, J. R. Cheeseman, V. G. Zakrzewski, J. A. Montgomery, R. E. Stratmann, J. C. Burant, S. Dapprich, J. M. Millam, A. D. Daniels, K. N. Kudin, M. C. Strain, O. Farkas, J. Tomasi, V. Barone, M. Cossi, R. Cammi, B. Mennucci, C. Pomelli, C. Adamo, S. Clifford, J. Ochterski, G. A. Petersson, P. Y. Ayala, Q. Cui, K. Morokuma, D. K. Malick, A. D. Rabuck, K. Raghavachari, J. B. Foresman, J. Cioslowski, J. V. Ortiz, A. G. Baboul, B. B. Stefanov, G. Liu, A. Liashenko, P. Piskorz, I. Komaromi, R. Gomperts, R. L. Martin, D. J. Fox, T. Keith, M. A. Al-Laham, C. Y. Peng, A. Nanayakkara, M. Challacombe, P. M. W. Gill, B. G. Johnson, W. Chen, M. W. Wong, J. L. Andres, C. Gonzalez, M. Head-Gordon, E. S. Replogle, J. A. Pople, Gaussian, Inc., Pittsburgh, PA, **1998**.
- [35] F. Mohamadi, N. G. J. Richards, W. C. Guida, R. Liscamp, M. Lipton, C. Caufield, G. Chang, T. Hendrickson, W. C. Still, *J. Comput. Chem.* **1990**, *11*, 440–467.
- [36] R. G. Parr, W. Yang, *Density Functional Theory of Atoms and Molecules*, Oxford Science Publication, Oxford, **1989**.
- [37] A. D. Becke, *J. Chem. Phys.* **1993**, *98*, 5648–5652.
- [38] P. Hudáky, I. Jákly, A. G. Császár, A. Perczel, *J. Comput. Chem.* **2001**, *22*, 732–751.

Received: February 24, 2003 [F4881]